Chinese Chemical Letters 33 (2022) 1337–1342

Contents lists available at ScienceDirect

Chinese Chemical Letters

journal homepage: www.elsevier.com/locate/cclet

Degradation of tetracycline hydrochloride by ultrafine TiO_2 nanoparticles modified g-C_3N_4 heterojunction photocatalyst: Influencing factors, products and mechanism insight

Bin Zhang[a,b], Xu He[b], Chengze Yu[a], Guocheng Liu[a], Dong Ma[a], Chunyue Cui[a], Qinghua Yan[a], Yingjie Zhang[c], Guangshan Zhang[a], Jun Ma[a,b], Yanjun Xin[a,*]

[a] Qingdao Engineering Research Center for Rural Environment, Water Resources Protection and Utilization Center for Rural Areas, Qingdao Agricultural University, Qingdao 266109, China
[b] State Key Laboratory of Urban Water Resource and Environment, Harbin Institute of Technology, Harbin 150090, China
[c] School of Marine Science and Technology, Sino-Europe Membrane Technology Research Institute Harbin Institute of Technology, Weihai 264209, China

ARTICLE INFO

Article history:
Received 9 May 2021
Revised 19 July 2021
Accepted 4 August 2021
Available online 10 August 2021

Keywords:
Photocatalytic
TiO_2
G-C_3N_4
Tetracycline hydrochloride
Mechanism

ABSTRACT

The unique heterojunction photocatalyst of graphite carbon nitride (g-C_3N_4) modified ultrafine TiO_2 (g-C_3N_4/TiO_2) was successfully fabricated by electrochemical etching and co-annealing method. However, the effects of various environmental factors on the degradation of TC by g-C_3N_4/TiO_2 and the internal reaction mechanism are still unclear. In this study, the effects of initial pH, anions, and cations on the photocatalytic degradation of tetracycline hydrochloride (TC) by g-C_3N_4/TiO_2 were systematically explored, and the scavenging experiment and intermediate detection were conducted to better reveal the mechanism on photocatalytic degradation of TC. The results showed that the removal efficiency of photocatalytic degradation of TC by g-C_3N_4/TiO_2 could reach 99.04% under Xenon lamp irradiation within 120 min. The unique g-C_3N_4/TiO_2 heterojunction photocatalyst showed excellent photocatalytic performance for the degradation of TC at pH 3∼7, and possesses outstanding anti-interference ability to NO_3^-, Cl^-, Na^+, Ca^{2+} and Mg^{2+} ions in natural waters during the photocatalytic degradation TC process. Superoxide radicals ($O_2^{\bullet-}$) and hydroxyl radicals ($^{\bullet}OH$) were proved as the main reactive species for TC degradation, and the possible mechanism of the unique photocatalytic system for g-C_3N_4/TiO_2 was also proposed. The above results can provide a reliable basis and theoretical guidance for the design and application of visible photocatalyst with high activity to degrade the actual wastewater containing TC.

Antibiotics, as one of the great medical achievements in the 20th century, have greatly prolonged the life span of human beings [1]. In recent years, antibiotics were widely used in healthcare, animal husbandry, and agriculture for their ability to control and treat infectious diseases [2–4]. However, the problem of water pollution caused by the abuse of antibiotics is becoming more and more serious, which has attracted the attention of researchers [5]. For example, tetracycline is easily stored and accumulated in the aquatic environment due to its high solubility [6]. Furthermore, it is difficult to be biodegraded in the environment because most tetracycline is discharged in its original form after metabolism in the body [7]. Thus, tetracycline is one of the main sources of antibiotic pollution in the environment. Moreover, tetracycline residues belong to persistent organic pollutants, which could pollute the water environment and cause great damage to human health. Hence, it is an important mission of researchers to search for effective methods to remove it from water.

At present, the treatment of wastewater containing tetracycline residue mainly includes the following methods: adsorption [8,9], biological treatment [10], and chemical treatment [4,11]. However, tetracycline cannot be completely decomposed by the adsorption method, which can easily cause secondary pollution to the environment. The degradation of tetracycline by the single biological treatment has a relatively long period and the effluent cannot reach the standard without other additional methods [12]. Some conventional chemical treatments are expensive because they require large amounts of chemicals. Photocatalytic oxidation technology is considered as an ideal way to remove antibiotics from water, which has the advantages of solar energy utilization, mild reaction conditions, strong oxidation ability, and stable performance [13–16]. Furthermore, it can mineralize antibiotics into CO_2 and

* Corresponding author.
E-mail address: xintom2000@126.com (Y. Xin).

https://doi.org/10.1016/j.cclet.2021.08.008
1001-8417/

H_2O without secondary pollution [17–19]. During the past decades, TiO_2 semiconductor is considered as a promising photocatalyst for its non-toxic, high stability, and low cost [20–22]. And the ultrafine TiO_2 nanoparticles have more excellent photocatalytic activity compared with P25 due to their more active sites and quantum size effects [23]. However, the low visible light absorption of TiO_2 limits its further practical applications, which is caused by the wide band gap (3.2 eV) [24]. Meanwhile, the photocatalytic quantum efficiency of single ultrafine TiO_2 nanoparticles is still limited due to the recombination of photo-electrons and holes. To further improve the visible-light photocatalytic activity and inhibit the recombination of photo-electrons and holes of ultrafine TiO_2 nanoparticles, the combination of semiconductors is considered as a valid strategy [25,26]. At the same time, g-C_3N_4 as a non-metal material with a narrow bandgap width (2.7 eV) has also attracted extensive attention from researchers due to its high utilization rate of visible light (∼460 nm) [27–29]. However, it also exists a fatal defect that the photogenic carriers of g-C_3N_4 are easily recombined, resulting in low photocatalytic activity [30]. To promote the utilization of visible light and further improve the photocatalytic performance of ultrafine TiO_2 nanoparticles, we have successfully designed and constructed a novel unique heterojunction photocatalyst of ultrafine TiO_2 nanoparticles modified g-C_3N_4 (g-C_3N_4/TiO_2) with high visible light photocatalytic activity [23]. The unique heterojunction photocatalyst system, can not only promote the separation of photogenerated carriers but also improve the utilization rate of visible light, demonstrated excellent photocatalytic performance. However, the photocatalytic degradation performance of g-C_3N_4/TiO_2 for tetracycline hydrochloride (TC) under different solution factors has not been revealed. The detailed photocatalytic reaction mechanism, such as the active species and its transformation pathway, and the possible intermediate of TC, is unknown, which will hinder the efficient treatment of TC wastewater in practical application.

In practical wastewater containing antibiotics, the photocatalytic process is also affected by various factors, such as initial pH, anions, cations [31,32]. For example, the charge on the surface of photocatalyst and the form of the pollutant will also be influenced by solution pH, which will also affect the adsorption of TC on the surface of photocatalyst and some active radicals reaction [33]. In addition, the inorganic ions will also participate in the process of photocatalysis through various ways, such as reacting with radicals, competing for adsorption with pollutants, which could further affect the photocatalytic activity of the system [34]. Thus, the influencing factors and reaction mechanism of TC degradation by the unique g-C_3N_4/TiO_2 system were devoid in further exploration. Clarifying the role of influencing factors on the degradation of TC can provide better theoretical guidance for the practical treatment of TC in wastewater. Meanwhile, it is of great significance to further reveal the photocatalytic degradation mechanism of TC on g-C_3N_4/TiO_2, which will contribute to better understand the nature of photocatalytic degradation reactions. Therefore, it is of great value to study the effects of various factors on photocatalytic degradation of TC by the unique g-C_3N_4/TiO_2 system.

In the present work, the microstructure of g-C_3N_4/TiO_2 composite materials was characterized by a high-resolution transmission electron microscope (HR-TEM) and selected area electron diffraction (SAED). The effects of initial pH, anions, and cations on photocatalytic degradation of TC were further investigated and analyzed, so were the radical quenching agents, such as benzoquinone, tert–butyl alcohol, ammonium oxalate, and Fe(II)-ethylene diamine tetraacetic acid; and the unique conduction system and photocatalytic degradation mechanism of TC by g-C_3N_4/TiO_2 were proposed. This work can provide a theoretical basis and important reference value for the photocatalytic treatment of tetracycline pollution in water.

The specific datils of experiments were in Supporting information (Text S1 in Supporting information). The morphology and structural composition of g-C_3N_4/TiO_2 were characterized by TEM, HR-TEM, and SADE (Fig. 1). As shown in Fig. 1a, the flaky outline structure and the black granular substance were g-C_3N_4 and ultrafine TiO_2, respectively. It was apparent that the 2D lamellar structure of g-C_3N_4 was combined with ultrafine TiO_2 nanoparticles (Fig. 1a), and the HR-TEM images showed that the lattice spacing was 0.35 nm and 0.326 nm corresponds to (101) crystal surface of anatase TiO_2 and (002) crystal surface of g-C_3N_4, respectively. The heterojunction interface was formed by the combination of TiO_2 and g-C_3N_4, which indicated that the g-C_3N_4/TiO_2 composites were successfully synthesized (Fig. 1b). In addition, it could be seen that g-C_3N_4/TiO_2 composites possess a polycrystalline structure (Fig. 1c), which could further confirm the successful formation of composite photocatalysts.

The pH value of aqueous solution plays an important role in the photocatalytic degradation of organic pollutants [35], and the isoelectric point of photocatalytic materials is a significant parameter for the adsorption process of organic pollutant [36]. The change of zeta potential of g-C_3N_4/TiO_2 with pH values of aqueous solution is shown in Fig. 2a. The isoelectric point value of g-C_3N_4/TiO_2 was determined to be about 3. When the pH of the solution is less than 3, the surface of g-C_3N_4/TiO_2 would be positively charged; and when it was greater than 3, the surface of the material will be negatively charged. As shown in Fig. 2b, the species distribution of TC would change with pH values because pH could change the chemical structure of TC in aqueous solution [33]. Fig. 2c showed the effect of different pH values on photocatalytic degradation efficiency of TC. It could be seen that the removal efficiency of TC could reach more than 80% when the pH value is between 3∼8, while it was significantly decreased when pH decreased to 1. Furthermore, the removal efficiency of TC also decreased gradually as the pH > 7. The above results indicated that the photocatalytic degradation of TC by g-C_3N_4/TiO_2 was not promoted under strong acidic and alkaline conditions. The main reasons for the phenomena were as follows: (1) The surface of g-C_3N_4/TiO_2 is positively charged at pH 1, and the main species form of TC is TCH_3^+. Therefore, the photocatalytic degradation efficiency of TC will be significantly inhibited due to the inefficient adsorption of TCH_3^+ to the positively charged surface of g-C_3N_4/TiO_2. In addition, a large number of H^+ will produce competitive adsorption with TCH_3^+. (2) When pH at 3.3∼7.7, TC is present as TC^0 molecule. The adsorption resistance between g-C_3N_4/TiO_2 and TC is weakened, and the active sites on the surface of g-C_3N_4/TiO_2 are fully utilized, which promotes the adsorption of TC on the photocatalyst surface. (3) Decrease of the photocatalytic efficiency of TC, when pH > 7.7, is also due to the inefficient adsorption of the negatively charged form of TC (TCH^- and TCH^{2-}) on the negatively charged surface of g-C_3N_4/TiO_2. However, under alkaline conditions, it is conducive to the formation of hydroxyl radicals ($^{\bullet}OH$) as active species (Eq. 1) [37], so the photocatalytic efficiency is not as low as that of pH 1.

$$OH^- + h^+ \rightarrow {}^{\bullet}OH \quad (1)$$

Anions such as NO_3^-, Cl^-, HCO_3^- and SO_4^{2-} are commonly present in the practical antibiotic wastewater, which may react with photo-generated electron-hole pairs and active species to influence the photocatalytic degradation rate of TC [34]. Therefore, it is necessary to study the effects of different anions on the photocatalytic reaction process. As shown in Fig. 2d, when the concentration of NO_3^- is relatively low (≤ 20 mmol/L), the photocatalytic degradation efficiency of TC showed an increasing trend with the increase of NO_3^- concentration. But when the concentration of Cl^- is not higher than 20 mmol/L, the photocatalytic degradation efficiency of TC presented a trend of first increasing and then decreas-

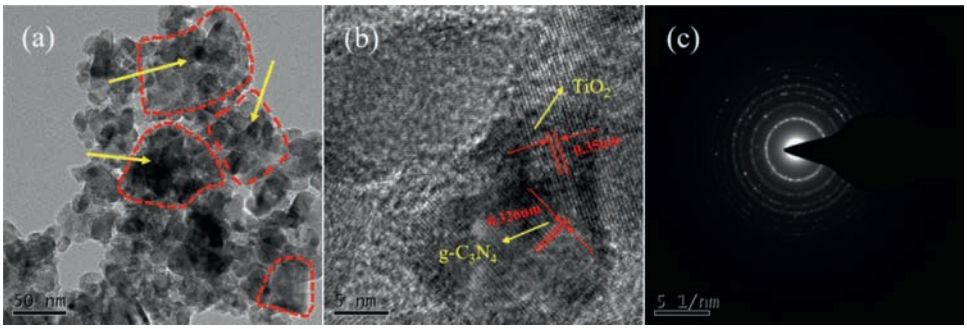

Fig. 1. TEM (a), HR-TEM (b) images, and selected area electron diffraction rings of (c) g-C_3N_4/TiO_2.

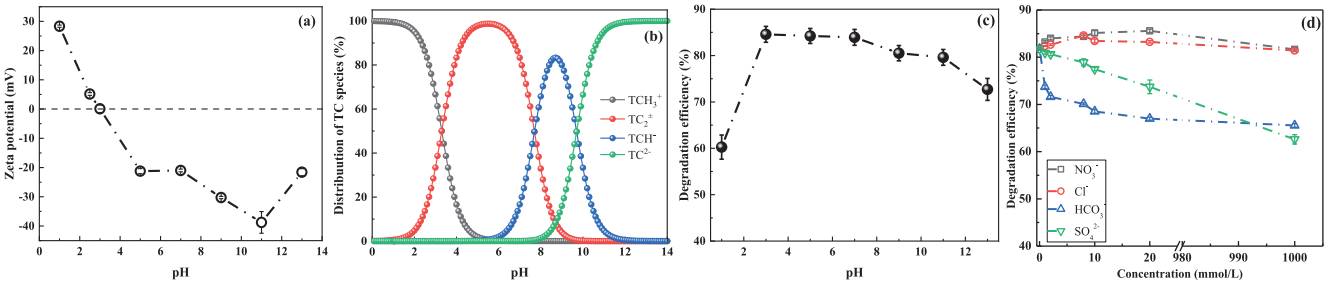

Fig. 2. (a) The zeta potentials of g-C_3N_4/TiO_2 change with the pH values of aqueous solution. (b) The distribution of TC species as a function of the pH values of aqueous solution. (c) The effect of pH values on photocatalytic degradation of TC. (d) Photocatalytic degradation efficiency of TC by g-C_3N_4/TiO_2 in the presence of different concentrations of NO_3^-, Cl^-, HCO_3^- and SO_4^{2-}.

ing. Besides, it was observed that with ion concentrations of NO_3^- and Cl^- as high as 1000 mmol/L, the photocatalytic degradation efficiency only decreased by 0.10% and 0.34%, respectively; and it can be seen that the effect of NO_3^- and Cl^- on the photocatalytic removal of TC by g-C_3N_4/TiO_2 was negligible. It is worth mentioning that sodium salts ($NaNO_3$ and NaCl) were used to study the effects of the ions on photocatalytic degradation of TC in this work, which could be inferred that Na^+ has little interference effect on the photocatalytic system. For HCO_3^- and SO_4^{2-}, the inhibitory effect of photocatalytic removal of TC was continuously expanded with the increase of ions concentrations, and the photocatalytic degradation efficiency of TC decreased by 16.21% and 19.15% in the presence of 1000 mmol/L HCO_3^- and SO_4^{2-}, respectively. These results indicated that the g-C_3N_4/TiO_2 has strong anti-interference ability for NO_3^-, Cl^- and Na^+ ions during the photocatalytic degradation of TC, which will be beneficial to deal with practical antibiotic wastewater.

In particular, for NO_3^-, it can absorb ultraviolet light to produce $^{\bullet}OH$ Eqs. 2 and 3 [38] to promote the photocatalytic activity [39], so the photocatalytic degradation efficiency showed a weak promoting effect at a low NO_3^-concentration Fig. 2d); meanwhile $^{\bullet}OH$ could also be captured by NO_2^- (Eq. 4), resulting in almost no effect for the photocatalytic performance of g-C_3N_4/TiO_2 at a high concentration of NO_3^-. For Cl^-, the chlorine radicals ($Cl^{\bullet}$) are formed through oxidization of Cl^- by $^{\bullet}OH$ and h^+ Eqs. 5 and 6, and could further transfer to Cl_2 (Eq. 7). On the one hand, the molecular structure of TC contains several electron-rich groups which are more vulnerable to attack by Cl_2 [40], which will be beneficial to the improvement of the photocatalytic degradation efficiency of TC. However, on the other hand, the oxidation property of Cl_2 (E_0 (Cl_2/2Cl^-) = 1.36 V) is weaker than that of $^{\bullet}OH$ (E_0 = 2.8 V) [41], so the enhancement of TC degradation with the increase of chloride ion concentration of Cl^- is not prominent. For the HCO_3^-, active species h^+ and $^{\bullet}OH$ could react with HCO_3^- and CO_3^{2-} to generate carbonate radical ($CO_3^{\bullet-}$) (Eqs. 8–12). However, the oxidation capacity of $CO_3^{\bullet-}$ is extremely weak [42], leading to a significant decrease in photocatalytic degradation of TC; h^+ and $^{\bullet}OH$ are also consumed to produce sulfate radicals ($SO_4^{\bullet-}$) Eqs. 13 and 14, $SO_4^{\bullet-}$ are also less oxidizing than h^+ and leads to a decrease in photocatalytic efficiency. In addition, anions could compete with TC to occupy active sites and thus inhibit photocatalytic activity [43]. To enhance the ability of the system to treat antibiotics in a wide variety of ions, we will enhance the anti-interference capability of the system to SO_4^{2-} and HCO_3^- by further optimizing the unique g-C_3N_4/TiO_2 heterojunction photocatalyst in future studies.

$$NO_3^- + h\nu \rightarrow NO_2^- + O^{\bullet-} \quad (2)$$

$$O^{\bullet-} + H_2O \rightarrow {}^{\bullet}OH + OH^- \quad (3)$$

$$NO_2^- + {}^{\bullet}OH \rightarrow OH^- + NO_2 \quad (4)$$

$$Cl^- + {}^{\bullet}OH \rightarrow Cl^{\bullet} + OH^- \quad (5)$$

$$Cl^- + h^+ \rightarrow Cl^{\bullet} \quad (6)$$

$$Cl^{\bullet} + Cl^{\bullet} \rightarrow Cl_2 \quad (7)$$

$$HCO_3^- + OH^- \rightleftarrows H_2O + CO_3^{2-} \quad (8)$$

$$HCO_3^- + {}^{\bullet}OH \rightarrow CO_3^{\bullet-} + H_2O \quad (9)$$

$$HCO_3^- + h^+ \rightarrow CO_3^{\bullet-} \quad (10)$$

$$CO_3^{2-} + {}^{\bullet}OH \rightarrow CO_3^{\bullet-} + H_2O \quad (11)$$

$$CO_3^{2-} + h^+ \rightarrow CO_3^{\bullet-} \quad (12)$$

$$SO_4^{2-} + h^+ \rightarrow SO_4^{\bullet-} \quad (13)$$

$$SO_4^{2-} + {}^{\bullet}OH \rightarrow SO_4^{\bullet-} + OH^- \quad (14)$$

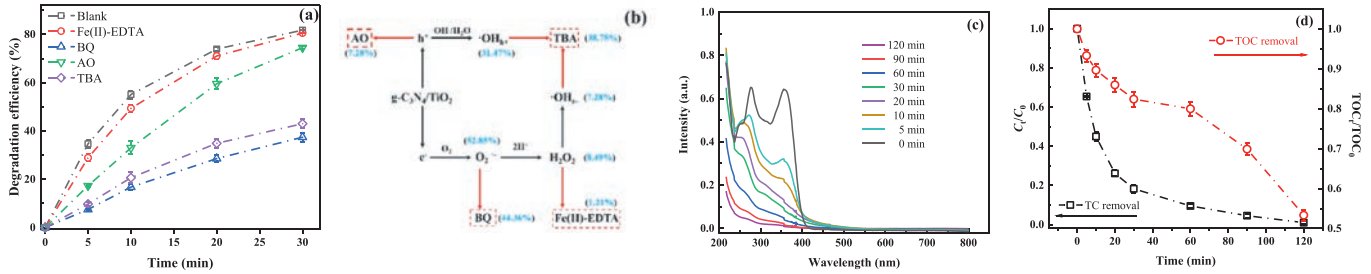

Fig. 3. (a) Photocatalytic degradation efficiency of TC by g-C_3N_4/TiO_2 in the presence of different scavengers and (b) the contribution of various active radicals. (c) The full wavelength absorption scan spectrum of TC and (d) TOC removal rate by g-C_3N_4/TiO_2 at different time.

The effects of typical cations, Ca^{2+} and Mg^{2+}, on the degradation efficiency of TC were shown in Table. S1. Clearly, with the increase of concentration of Ca^{2+} and Mg^{2+}, the degradation efficiency of TC by g-C_3N_4/TiO_2 showed an inconspicuous trend of increase and then decrease. Here the effects of both Cl^- and cations ($Ca^{2+}$and Mg^{2+}) should be taken into account, as shown in Fig. 2d, the low concentration of Cl^- has a certain promotion effect on the photocatalytic degradation of TC, but the effect of Cl^- is negligible at 1000 mmol/L. The degradation efficiency was reduced by only 5.58% and 4.47% in the presence of 1000 mmol/L Ca^{2+} and Mg^{2+} compared to the absence of excess ions. These results showed that the g-C_3N_4/TiO_2 also has strong anti-interference for Ca^{2+} and Mg^{2+}, which could be explained by the following reasons: (1) Similar to the influence of Cl^- mentioned above, $Cl^{\bullet}$ generated by Cl^- are more likely to react with electron-rich TC and thus improve the photocatalytic performance of TC. (2) The solubility product constant of $Ca(OH)_2$ and $Mg(OH)_2$ is relatively small, which will be prone to precipitate at higher concentrations of Ca^{2+} and Mg^{2+} Eqs. 15 and 16 [44,45]. The formation of suspension that will hinder the utilization of visible light by photocatalyst to reduce the photocatalytic activity of g-C_3N_4/TiO_2, which could offset the improvement of photocatalytic degradation effect caused by cations, showing a slight inhibitory effect on the whole system.

$$Ca^{2+} + 2OH^- \rightarrow Ca(OH)_2 \downarrow K_{sp} = 5.5 \times 10^{-6} \quad (15)$$

$$Mg^{2+} + 2OH^- \rightarrow Mg(OH)_2 \downarrow K_{sp} = 1.2 \times 10^{-11} \quad (16)$$

In the photocatalytic degradation system, the existence of active substances is considered to be the crucial factor for organic pollutant degradation [46]. Meanwhile, based on the results and discussion mentioned above, the effects of pH and ions on the photocatalytic degradation efficiency of TC are also closely related to active radicals. In order to reveal the role of active species in photocatalytic degradation of TC by g-C_3N_4/TiO_2, the trapping experiment was performed by adding various active species scavengers [47]. The concentrations of BQ, TBA, AO, and Fe(II)-EDTA were 1 mmol/L to capture the active species $O_2^{\bullet-}$,$^{\bullet}OH$, h^+, and H_2O_2, respectively. As shown in Fig. 3a, the photocatalytic degradation efficiency of TC by g-C_3N_4/TiO_2 decreased from 81.76 to 80.55% in the presence of Fe(II)-EDTA within 30 mins, indicating that H_2O_2 demonstrated a slight effect on the photocatalytic removal of TC. With the existence of AO, the photocatalytic degradation efficiency of TC by g-C_3N_4/TiO_2 decreased by 8.9%, indicating that the h^+ contributed to photocatalytic degradation TC. The photocatalytic efficiency of TC decreased by 38.75% and 44.36% in the presence of TBA and BQ, respectively, which confirmed that both $O_2^{\bullet-}$ and $^{\bullet}OH$ played dominant roles in photocatalytic degradation of TC. Furthermore, the contribution of $O_2^{\bullet-}$ was higher than that of $^{\bullet}OH$, which verified that the strong anti-ion interference ability of the system was mainly due to the strong selectivity of $O_2^{\bullet-}$ radicals and their difficulty in quenching.

In order to further understand the contribution of various radicals in the process of photocatalytic degradation of TC by g-C_3N_4/TiO_2, the transformation of various radicals and the corresponding essential functions are revealed as shown in Fig. 3b. It can be seen that the direct contribution rate of h^+ in the process of TC degradation accounts for 7.28%. The contribution rates of $O_2^{\bullet-}$ and $^{\bullet}OH$ radicals directly acting on the TC degradation are 44.36% and 38.75%, respectively. The h^+ will react with H_2O and OH^- to form $^{\bullet}OH_{h^+}$ radicals, and H_2O_2 breaks down into $^{\bullet}OH_{e^-}$ radicals under the simulated sunlight irradiation, which two components are the total contribution of $^{\bullet}OH$ radicals to photocatalytic degradation process. In addition, 8.49% of $O_2^{\bullet-}$ radicals react with H^+ to generate H_2O_2 except that 44.36% of $O_2^{\bullet-}$ radicals were directly acting on the photocatalytic degradation of TC. Furthermore, H_2O_2, which accounts for 1.48%, can directly act on the degradation of TC. The above results in conformity with the activity radicals scavenging experiment (Fig. 3a).

The intermediate products produced during the photocatalytic degradation of TC were detected by LC-MS spectra. Twenty-one kinds of possible intermediate products were found through analyzing the corresponding mass-to-charge ratios (*m/z*) and their structure information was shown in Table S2 (Supporting information). According to the above results, the possible photocatalytic degradation pathways of TC by g-C_3N_4/TiO_2 could be speculated (Fig. S1 in Supporting information). Through radical scavenging experiments, we have concluded that $O_2^{\bullet-}$ and $^{\bullet}OH$ play the significant roles in the photocatalytic degradation of TC system (Figs. 3a and b). $O_2^{\bullet-}$ have good oxidability and reducibility, which can react with the target. Besides, the nucleophilic properties of $O_2^{\bullet-}$ can promote the degradation of target pollutants [48]. The $^{\bullet}OH$ has strong oxidizing ability and electrophilicity [42], which can break the bonds of the target and produce electrophilic addition reactions, respectively. As shown in Fig S1, the possible reaction pathways of TC in the photocatalytic process are mainly divided into two parts. (1) In pathway I, TC could react with $^{\bullet}OH$ radical to form **P19** (*m/z* 469) accompanied by hydroxylation, and *N*-methyl (CH_3) is oxidized to the *N*-aldehyde (CH=O) group under the action of $^{\bullet}OH$ radical, which is consistent with other reports [49]. But interestingly, **P20** (*m/z* 475) will react with the $^{\bullet}OH$ radical to form **P21** (*m/z* 491) in the electrophilic addition reaction. (2) In pathway II, TC will forms **P1** (*m/z* 427) by losing an H_2O molecule under the action of $O_2^{\bullet-}$ and $^{\bullet}OH$ radical [11]. In addition, TC will break the $-CH_3$ and =O bonds under attack by $O_2^{\bullet-}$ and $^{\bullet}OH$ radical, which will produce **P2** (*m/z* 413) and **P3** (*m/z* 412), respectively. Next, **P1** (*m/z* 417) will generate **P4** (*m/z* 413) and **P8** (*m/z* 384) by further demethylation and deamination, respectively. And **P8** (*m/z* 384) will generate **P9** (*m/z* 294) by ring-opening reaction under the action of h^+, $O_2^{\bullet-}$ and $^{\bullet}OH$. On the other hand, under the attack of $O_2^{\bullet-}$ and $^{\bullet}OH$ radicals, **P5** (*m/z* 399) are generated by **P4** take off a methyl group due to the low bond energy of N–C [50]. And **P5** will continue to lose methyl, amino groups, and aldehyde groups to form **P6**

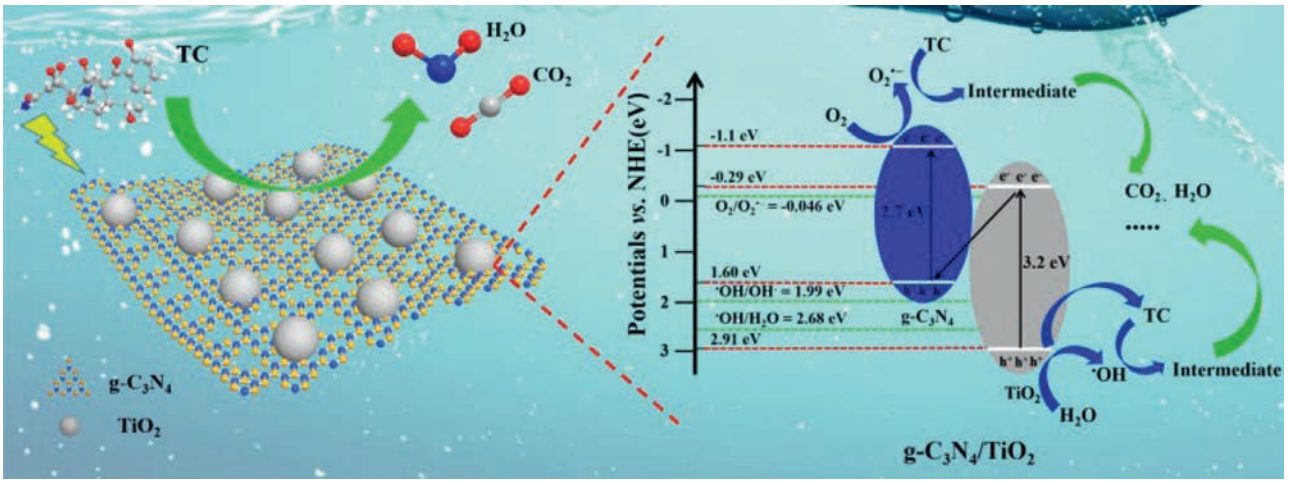

Fig. 4. The proposed mechanism for photocatalytic degradation of TC by g-C_3N_4/TiO_2.

(*m/z* 355) and **P7** (*m/z* 328). In addition, **P11** (*m/z* 318) and **P10** (*m/z* 301) [51] were generated by a series of bond breaking and ring-opening reactions under the attack of various radicals. Among them, the double bond was vulnerable to oxidizing agents, which cause an open-loop reaction of **P7** (*m/z* 328) to form **P11** (*m/z* 318) [11]. In particular, **P10** (*m/z* 301) also introduces −OH groups to form **P11** when the two methyl groups were removed. Furthermore, **P12** (*m/z* 231) will generate **P13** (*m/z* 215) *via* dehydroxylation, **P13** will generate **P14** (*m/z* 177) *via* ring-opening reaction, **P14** will generate **P15** (*m/z* 163) *via* demethylation reaction, **P15** will generate **P16** (*m/z* 149) via aldehyde bond removal. And **P17** (*m/z* 121) was produced by **P16** through an open-loop reaction, which is different from the formation path of **P17** reported in the literature [50]. The breaking of the double bond of **P17** and the breaking of the benzene ring led to the formation of **P18** (*m/z* 101). In the end, **P18** will be mineralized to CO_2 and H_2O by various active radicals. In summary, after a series of reactions including hydroxylation, electrophilic addition, nucleophilic substitution, redox reaction, demethylation, deaminize, dealdehyde and ring-opening reaction, TC will be degraded into some intermediates and further generate CO_2, H_2O, and some small molecule.

The full wavelength absorption scan spectrum of TC solution by g-C_3N_4/TiO_2 was measured at different times. As shown in Fig. 3c, it could be clearly seen that the absorption peaks strength of TC solution decreased with the increase of time, and TC was almost absolutely degraded by photocatalytic after 120 mins simulated solar illumination. At the same time, the TC and TOC removal rate by g-C_3N_4/TiO_2 were investigated (Fig. 3d). Obviously, after 120 mins photocatalytic degradation, the degradation efficiency of TC could reach 99.04%, which is consistent with Fig. 3c. Meanwhile, the TOC removal rate could reach 46.69% under the photocatalytic degradation of 120 min, which suggests that part of TC is degraded to intermediate, part of the TC is completely mineralized into CO_2 and H_2O. However, the decrease rate of TOC was relatively slow at 40–60 min, which may be caused by the difficult degradation and mineralization of macromolecular organic matter generated during this period. According to the above results, we could deduce the conclusion that $O_2^{\bullet-}$ and $^{\bullet}OH$ radicals are the main reactive species in the photocatalytic degradation of TC by g-C_3N_4/TiO_2 system, which corresponds to the results of active species capture experiments (Fig. 3a). Especially, the photocatalytic degradation pathway of TC by g-C_3N_4/TiO_2 is unique, which is clearly different from other technologies [50,52] and photocatalytic systems [53,54].

According to the above experimental results, the charge transfer mechanism between TiO_2 and g-C_3N_4, and the process for photocatalytic degradation of TC by g-C_3N_4/TiO_2 heterojunction photocatalyst were presented in Fig. 4. The VB electrons of both g-C_3N_4 and TiO_2 are excited into the CB under simulated sunlight irradiation (Eqs. 17 and 18). The CB of g-C_3N_4 is more negative (−1.1 eV *versus* NHE) [55] than that of TiO_2 (−0.29 eV *versus* NHE) and $E_0 = O_2/O_2^{\bullet-}$ (−0.046 eV *versus* NHE), it will be more conducive to reaction for O_2 with e^-. The VB of TiO_2 is more positive (2.91 eV *versus* NHE) [55] than $E_0 = {}^{\bullet}OH/OH^-$ (1.99 eV *versus* NHE) and $E_0 = {}^{\bullet}OH/H_2O$ (2.68 eV *versus* NHE), which will be more conducive to the reaction of h^+ and H_2O/OH^- to form active radicals. Especially, the VB of g-C_3N_4 (1.6 eV *versus* NHE) is lower than that of $E_0 = {}^{\bullet}OH/OH^-$ (1.99 eV *versus* NHE) and $E_0 = {}^{\bullet}OH/H_2O$ (2.68 eV *versus* NHE), resulting in insufficient oxidation capacity of holes and could not to generate $^{\bullet}OH$ radicals. Thus, O_2 could combine with electrons in the CB of g-C_3N_4 to form $O_2^{\bullet-}$ radicals (Eq. 19), H_2O and OH^- also react with h^+ of TiO_2 to generate $^{\bullet}OH_{h+}$ radicals (Eq. 21). In addition, $O_2^{\bullet-}$ radical can form H_2O_2 to further produce $^{\bullet}OH_{e-}$ radicals (Eq. 20). Based on the above analysis, a unique semiconductor system could be established between g-C_3N_4 and TiO_2. On the other hand, the electrons in the CB of TiO_2 will recombine with the h^+ in the VB of g-C_3N_4 by the heterogeneous junction interface (Fig. 1), which can further promote the formation of the unique heterostructure. This charge transfer conduction pathway between two semiconductors can eventually lead to the unique photocatalytic mechanism, and this constructed unique heterostructure photocatalytic system can not only promote the improvement of photocatalytic performance due to the inhibition of photon-generated carrier recombination, but also generate more active species of $O_2^{\bullet-}$ and $^{\bullet}OH$ radicals (Eqs. 19 and 21). The above-mentioned unique mechanism is consistent with the active radical scavenging experiment (Figs. 3a and b). Then, under the action of $O_2^{\bullet-}$, $^{\bullet}OH$ and h^+, TC is firstly decomposed into intermediate products, and then further mineralized into CO_2, H_2O, and other small molecular substances (SMS) (Eq. 22).

$$TiO_2 + h\nu \rightarrow h^+ + e^- \quad (17)$$

$$g\text{-}C_3N_4 + h\nu \rightarrow h^+ + e^- \quad (18)$$

$$O_2 + e^- (g\text{-}C_3N_4) \rightarrow O_2^{\bullet-} \quad (19)$$

$$O_2^{\bullet-} + 2H^+ \rightarrow H_2O_2 \rightarrow \ldots\ldots \rightarrow {}^{\bullet}OH_{e-} \quad (20)$$

$$H_2O/OH^- + h^+ (TiO_2) \rightarrow {}^{\bullet}OH_{h+} \quad (21)$$

$$TC + h^+ (TiO_2)/{}^{\bullet}OH/O_2^{\bullet-} \rightarrow \text{intermediate} \rightarrow CO_2 + H_2O + SMS \quad (22)$$

In conclusion, the photocatalytic degradation of TC was systematically studied by ultrafine TiO_2 nanoparticles modified g-C_3N_4 heterojunction photocatalyst. The g-C_3N_4/TiO_2 exhibited remarkable photocatalytic activity for the degradation of TC at pH 3–7, and the photocatalytic degradation of TC could be inhibited at pH < 3 and pH > 7. The unique g-C_3N_4/TiO_2 heterojunction photocatalyst has demonstrated excellent resistance to interference from most ions such as NO_3^-, Cl^-, Na^+, Ca^{2+}, and Mg^{2+} in the process of photocatalytic degradation of TC. And the photocatalytic degradation of TC could be significantly inhibited in the presence of HCO_3^- and SO_4^{2-}. $O_2^{\bullet-}$ and $^{\bullet}OH$ radicals were identified as the dominant active species in the unique heterojunction photocatalytic system. The TC molecule was decomposed into intermediate products by a series of active radicals, which would be further mineralized into CO_2, H_2O, and some small molecular substances. In general, the unique g-C_3N_4/TiO_2 photocatalytic system has a wide range of pH values applicable and remarkable anti-interference ability of major ions in natural water. This research could provide a meaningful reference for the construction of photocatalyst reaction system, and offer a novel direction for the treatment of antibiotic wastewater.

Declaration of competing interest

The authors declare that they have no known competing financial interests or personal relationships that could have appeared to influence the work reported in this paper.

Acknowledgments

This work is financially supported by National Natural Science Foundation of China (Nos. 52070107, 51678323), Natural Science Foundation of Shandong Province (Nos. ZR2019MD012, ZR2017MEE026), Support Plan on Youth Innovation Science and Technology for Higher Education of Shandong Province (No. 2019KJD014) and Natural Science Foundation of Heilongjiang Province (No. B2015024).

Supplementary materials

Supplementary material associated with this article can be found, in the online version, at doi:10.1016/j.cclet.2021.08.008.

References

[1] A. Ezzariai, M. Hafidi, A. Khadra, et al., J. Hazard. Mater. 359 (2018) 465–481.
[2] M.C. Danner, A. Robertson, V. Behrends, J. Reiss, Sci. Total Environ. 664 (2019) 793–804.
[3] X. Liu, D. Huang, C. Lai, et al., TrAC, Trends Anal. Chem. 109 (2018) 260–274.
[4] S. Xin, G. Liu, X. Ma, et al., Appl. Catal. B 280 (2021) 119386.
[5] Y. Wang, C. Zhou, J. Wu, J. Niu, Chin. Chem. Lett. 31 (2020) 2673–2677.
[6] H.M. Jang, E. Kan, Bioresour. Technol. 274 (2019) 162–172.
[7] D. Zhang, J. Yin, J. Zhao, H. Zhu, C. Wang, J. Environ. Chem. Eng. 3 (2015) 1504–1512.
[8] Y. Wang, X. Wang, J. Li, et al., Chem. Eng. J. 371 (2019) 366–377.
[9] Q. Song, Y. Fang, Z. Liu, et al., Chem. Eng. J. 325 (2017) 71–79.
[10] M. Cai, S. Ma, R. Hu, et al., Environ. Pollut. 242 (2018) 634–642.
[11] Y. Chen, Y. Ma, J. Yang, et al., Chem. Eng. J. 307 (2017) 15–23.
[12] H. Wang, J. Zhang, P. Wang, et al., Chin. Chem. Lett. 31 (2020) 2789–2794.
[13] M. Ge, J. Cai, J. Iocozzia, et al., Int. J. Hydrogen Energy. 42 (2017) 8418–8449.
[14] S. Ni, F. Han, W. Wang, D. Han, Y. Bao, et al., Sens. Actuator. B 259 (2018) 963–971.
[15] Z. Xing, J. Zhang, J. Cui, et al., Appl. Catal. B 225 (2018) 452–467.
[16] Q. Zhou, Z. Fang, J. Li, M. Wang, Microporous Mesoporous Mater. 202 (2015) 22–35.
[17] Z. Zhao, J. Fan, X. Deng, J. Liu, Chem. Eng. J. 360 (2019) 1517–1529.
[18] Y. Wang, F. He, L. Chen, et al., Chin. Chem. Lett. 31 (2020) 2668–2672.
[19] M. Chen, J. Yao, Y. Huang, H. Gong, W. Chu, Chem. Eng. J. 334 (2018) 453–461.
[20] H. Dong, G. Zeng, L. Tang, et al., Water Res. 79 (2015) 128–146.
[21] R. Hao, G. Wang, H. Tang, et al., Appl. Catal. B 187 (2016) 47–58.
[22] K. Sridharan, E. Jang, T.J. Park, Appl. Catal. B 142-143 (2013) 718–728.
[23] B. Zhang, X. He, X. Ma, et al., Sep. Purif. Technol. 247 (2020) 116932.
[24] Y. Huang, P. Wang, Z. Wang, et al., Appl. Catal. B 240 (2019) 122–131.
[25] Y. Huang, J. Zhang, Z. Wang, et al., Sol. RRL. 4 (8) (2020) 2000170.
[26] Y.F. Shen, C. Zhang, C.G. Yan, H.Q. Chen, Y.J. Zhang, Chin. Chem. Lett. 28 (2017) 1312–1317.
[27] R. Zhang, M. Ma, Q. Zhang, F. Dong, Y. Zhou, Appl. Catal. B 235 (2018) 17–25.
[28] Y. Xing, X. Wang, S. Hao, et al., Chin. Chem. Lett. 32 (2021) 13–20.
[29] Y. Wu, Q. Chen, S. Liu, et al., Chin. Chem. Lett. 30 (2019) 2186–2190.
[30] J. Ge, L. Zhang, J. Xu, et al., Chin. Chem. Lett. 31 (2020) 792–796.
[31] Y. Liu, X. He, X. Duan, Y. Fu, D.D. Dionysiou, Chem. Eng. J. 276 (2015) 113–121.
[32] G. Wang, Q. Zhang, Q. Chen, et al., Chem. Eng. J. 358 (2019) 1083–1090.
[33] T. Wu, Q. Xue, F. Liu, et al., Chem. Eng. J. 366 (2019) 577–586.
[34] A.M. Dugandžić, A.V. Tomašević, M.M. Radišić, et al., J. Photochem. Photobiol. A 336 (2017) 146–155.
[35] L. Xu, L. Yang, E.M.J. Johansson, Y. Wang, P. Jin, Chem. Eng. J. 350 (2018) 1043–1055.
[36] B. Zhu, P. Xia, W. Ho, J. Yu, Appl. Surf. Sci. 344 (2015) 188–195.
[37] J. Ma, C. Wang, H. He, Appl. Catal. B 184 (2016) 28–34.
[38] M.K. Kim, K.D. Zoh, Sci. Total Environ. 449 (2013) 95–101.
[39] Q. Zhang, N. Bao, X. Zhu, D. Ma, Y. Xin, J. Alloys Compd. 618 (2015) 761–767.
[40] X. Ao, W. Sun, S. Li, et al., Chem. Eng. J. 361 (2019) 1053–1062.
[41] J. Peng, X. Lu, X. Jiang, et al., Chem. Eng. J. 354 (2018) 740–752.
[42] G. Wang, Q. Chen, Y. Liu, et al., Chem. Eng. J. 337 (2018) 322–332.
[43] H. Eskandarloo, A. Badiei, M.A. Behnajady, Ind. Eng. Chem. Res. 53 (2014) 6881–6895.
[44] G. Qian, L. Feng, J.Z. Zhou, et al., Chem. Eng. J. 181-182 (2012) 251–258.
[45] W. Gao, Z. Li, Hydrometallurgy 117-118 (2012) 36–46.
[46] H. Wang, Y. Liang, L. Liu, J. Hu, W. Cui, J. Hazard. Mater. 344 (2018) 369–380.
[47] Q. Chen, Y. Xin, X. Zhu, Electrochim. Acta 186 (2015) 34–42.
[48] M. Hayyan, M.A. Hashim, I.M. AlNashef, Chem. Rev. 116 (2016) 3029–3085.
[49] M. Cao, P. Wang, Y. Ao, et al., J. Colloid Interface Sci. 467 (2016) 129–139.
[50] J. Cao, Z. Xiong, B. Lai, Chem. Eng. J. 343 (2018) 492–499.
[51] X. Liang, Y. Zhang, D. Li, et al., Appl. Surface Sci. 466 (2019) 863–873.
[52] J. Wang, D. Zhi, H. Zhou, X. He, D. Zhang, Water Res 137 (2018) 324–334.
[53] Y. Chen, K. Liu, Chem. Eng. J. 302 (2016) 682–696.
[54] Y. Zhang, J. Zhou, X. Chen, L. Wang, W. Cai, Chem. Eng. J. 369 (2019) 745–757.
[55] J. Zhang, S. Fang, J. Mei, et al., Sep. Purif. Technol. 194 (2018) 96–103.